

Hydroxyapatite Coatings on High Nitrogen Stainless Steel by Laser Rapid Manufacturing

ASHISH DAS^{1,4,5,6} and MUKUL SHUKLA^{1,2,3,7,8,9}

1.—Department of Mechanical Engineering, MNNIT, Allahabad, India. 2.—School of Mechanical and Aerospace Engineering, Queen's University, Belfast, Northern Ireland, UK. 3.—Department of Mechanical Engineering Technology, University of Johannesburg, Johannesburg, South Africa. 4.—School of Mechanical Engineering, KIIT University, Bhubaneswar, India. 5.—e-mail: ashishdas.1110@gmail.com. 6.—e-mail: ashish.dasfme@kiit.ac.in. 7.—e-mail: m.shukla@qub.ac.uk. 8.—e-mail: mukulshukla@mnnit.ac.in. 9.—e-mail: mshukla@uj.ac.za

In this research, the laser rapid manufacturing (LRM) additive manufacturing process was used to deposit multifunctional hydroxyapatite (HAP) coatings on high nitrogen stainless steel. LRM overcomes the limitations of conventional coating processes by producing coatings with metallurgical bond, osseointegration, and infection inhibition properties. The microstructure, microhardness, antibacterial efficacy, and bioactivity of the coatings were investigated. The microstructure studies established that the coatings consist of austenite dendrites with HAP and some reaction products primarily occurring in the inter-dendritic regions. A Vickers microhardness test confirmed the hardness values of deposited HAP coatings to be higher than those of the bare 254SS samples, while a fluorescence activated cell sorting test confirmed their superior antibacterial properties as compared with pristine samples. The coated samples immersed in simulated body fluid showed rapid apatite forming ability. The results obtained in this research signify the potential application of the LRM process in synthesizing multifunctional orthopaedic coatings.

INTRODUCTION

For joint replacements, orthopedic implants are frequently used and expected to rise for the next 15–20 years.¹ As reported previously, 18% of implants fail due to aseptic loosening while 20% fail because of infection.^{2,3} Hence, strong osseointegration and antibacterial properties both need to be taken into consideration while developing an implant material.⁴

Internal fixation devices are still being made of austenitic stainless steels (largely SS 316L) in spite of their lower corrosion resistance compared with titanium. This is a result of their excellent mechanical properties and low cost.^{5,6} Lately, a newer generation of steel UNS S31254 SS (254SS) has been studied. As reported in the literature, despite 254SS not being bioactive and lacking strong osseointegration, the absence of toxic effects and high nitrogen content of 254SS have made it a candidate for scientific investigation, in the hope of developing a futuristic orthopedic implant material.^{7,8}

Nevertheless, the literature confirms that these problems can be mitigated by depositing hydroxyapatite (HAP) coatings on metallic implants.^{9–17}

Hydroxyapatite (HAP) holds a significant position as an inorganic biomaterial, but bulk HAP ceramics possess poor mechanical properties restricting its use for non-load-bearing implant applications. To overcome this limitation, HAP is being coated on metals and their alloys to derive the advantages of both the bioactivity of HAP and the mechanical performance of metals.¹⁸ HAP is a widely used coating material for orthopedic implants because its mechanical properties closely match with those of human bone mineral, and it is also biocompatible with human bone tissues.¹⁹ HAP coating of orthopedic implants can be an effective method of improving their physiological response leading to an overall improved performance of the implants.²⁰

HAP coatings can be deposited on a metallic substrate using techniques such as direct laser melting, sol-gel, and vapor deposition processes,

including plasma spraying, which is a commercially viable technique for clinical applications.^{20–27} Nevertheless, HAP coatings produced by plasma-spray bond poorly with metal substrate and are a candidate to easy wear and tear, which results in undesirable debris formation.²⁸ Synthesizing a composite layer with HAP on the implant surface is one way to solve these problems. This can be achieved by melting the preplaced HAP on the implant surface using a laser.²⁴ The primary aim of this research is to assess the feasibility of synthesizing multifunctional orthopedic coatings on 254SS implant surfaces using laser rapid manufacturing (LRM), which can prevent infection while still promoting osseointegration. LRM is an additive manufacturing (AM) process, which can be used not only for preparing customized implants but also for treating their surfaces in several ways.^{24,29,30}

EXPERIMENTAL WORK

An LRM AM system equipped with a 2.0-kW continuous wave, Ytterbium-doped, fiber laser with a beam size of 2.5 mm was used. For direct laser melting of the preplaced HAP powder bed on the surface of a high nitrogen stainless steel (254SS) substrate ($100 \times 50 \times 2$ mm³ sheet), several coating samples, over a 10×10 mm² area, were prepared at 1000-W laser power and 1-m/min scan speed. These process parameter settings were finalized based on Refs. ²⁴ and ²⁵, and preliminary trials were conducted. At 800-W and 900-W laser power with 0.8-m/min, 0.9-m/min, and 1.0-m/min scan speeds, discontinuous tracks with weak bonding were produced. At 1000-W power with 0.8-m/min and 0.9-m/min scan speeds, discontinuous tracks were produced while 1200-W power with 0.8-m/min, 0.9-m/min, and 1.0-m/min scan speeds resulted in red hotness. These outcomes are undesirable for orthopedic coatings, and hence, the laser power and scan speed were finally fixed at 1000 W and 1 m/min, respectively.

The HAP-coated 254SS samples were sectioned and metallographically prepared for microstructural studies according to ASTM E3-11. Microstructure and surface morphology studies were conducted using an optical microscope and a scanning electron microscope (SEM, ZEISS EVO 50) equipped with an energy-dispersive spectrometer (EDS), respectively. The phase composition of the coated samples was examined using an x-ray diffraction (XRD; RIGAKU Model: Smart lab 3 KW). The microhardness of pristine and coated 254 stainless steel was determined using a Vickers microhardness tester. The antibacterial efficacy of pristine and coated 254 stainless steel samples was determined using the fluorescence activated cell sorting (FACS) technique, which is one of the best, modern technologies for cell sorting.³¹ Finally, the apatite-forming ability of the coated samples was determined by the simulated body fluid (SBF) immersion test. The samples were taken out from SBF after 2 days of immersion, washed with distilled water,

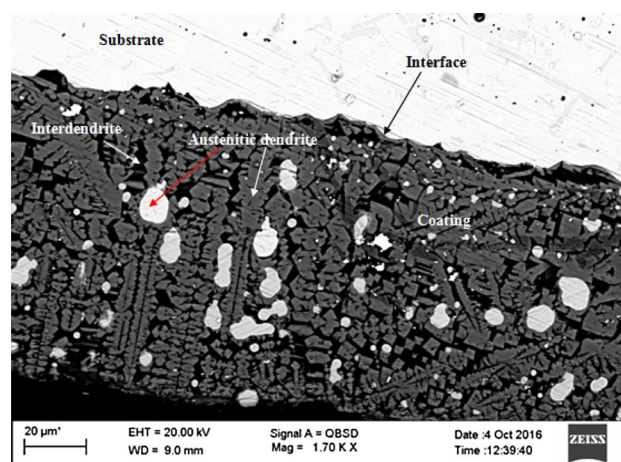


Fig. 1. SEM micrograph of the interface microstructure of the HAP-coated 254SS sample.

dried at 100°C, and then examined under SEM for apatite layer formation. It is believed that forming bone-like apatite in vitro is critical because apatite is the dominant inorganic phase of hard tissue. Thus, bone-like apatite formation indicates good osteoconductivity in biomaterials.³² Nevertheless, extensive in vivo studies are required to confirm the osseointegration, cytotoxicity, and biocompatibility of UNS S31254 stainless steel.

RESULTS AND DISCUSSION

Surface Morphology Characterization

In Figs. S1, S2 and S3 of the supplementary material, the cross sections of clad, heat-affected zone (HAZ), substrate, and successful deposition of coating on the substrate are clearly visible.

Figure 1 presents the SEM micrographs of the cross-sectional microstructure of the coated sample. Austenite dendrites and some interdendritic phases are clearly visible in the coated samples as shown in Fig. 1. The SEM micrograph of Fig. 1 confirms that the interface between HAP coating and the 254SS substrate is sound and diffused, which are the characteristics of the laser deposited coatings.^{29,30,33–35} Contrarily, HAP coatings deposited by other methods such as plasma spraying have a sharp interface, which is unacceptable for their long-term success.²⁹

A typical SEM microstructure image of the HAP-coated 254SS sample is shown in Fig. 2. Calcium is present in interdendritic phases, chromium is present in austenite dendrites phases, and iron is present in both austenite dendrites and interdendritic phases as clearly demonstrated in Fig. 2.

To acquire information about the composition and phase of the elements present in the deposited HAP coatings, EDS elemental mapping is carried out in this research. The EDS elemental mapping images of the HAP-coated 254SS sample are shown in Figs. S4, S5 and S6 of the supplementary material.

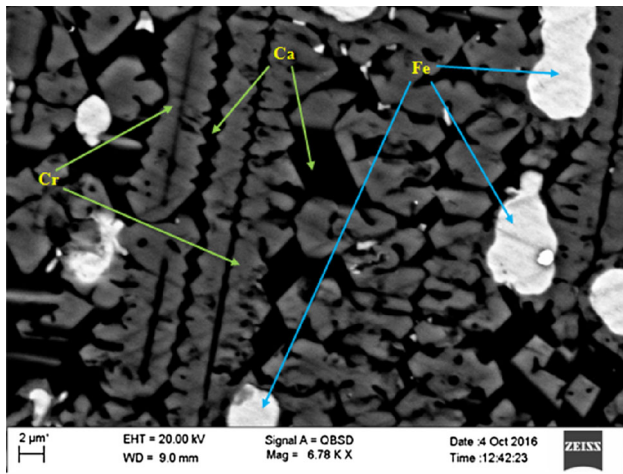


Fig. 2. SEM microstructure image of the HAP-coated 254SS sample.

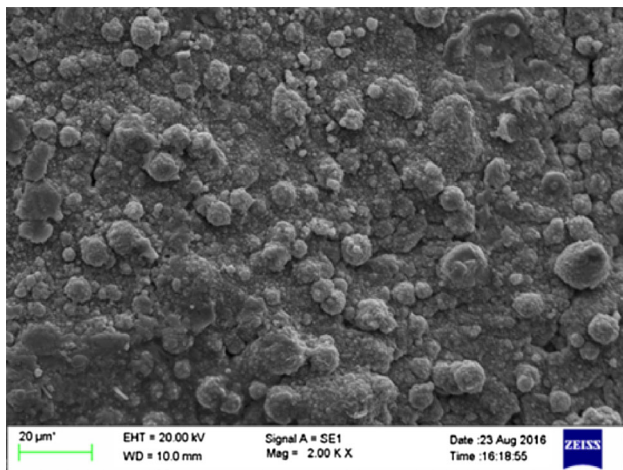


Fig. 3. SEM micrograph of the coated 254SS sample at 2000 times magnification.

The consistent surface morphology of the LRM-coated 254SS sample at 2000 times magnification is shown in Fig. 3.

The XRD diffractograms of the substrate, HAP powder, and HAP coating are presented in Fig. 4. The XRD results confirm the presence of HAP in crystalline format (2θ (31.66°, 34.48°, 35.98°, 39.04°, 47.26°, 56.58°, 62.74°, 64.44°) with minor traces of Fe_3P at 2θ (41.64°).

Microhardness

Microhardness tests were conducted to confirm the coatings' resistance to plastic deformation at a load of 300 g applied for 30 s as per Ref. ³⁶. The hardness of 504 ± 6 HV of HAP-coated 254SS substrate was found to be significantly higher than the hardness of the bare substrate 265 ± 14 HV, as confirmed by the difference in size of the indents in the optical micrograph of Fig. 5.

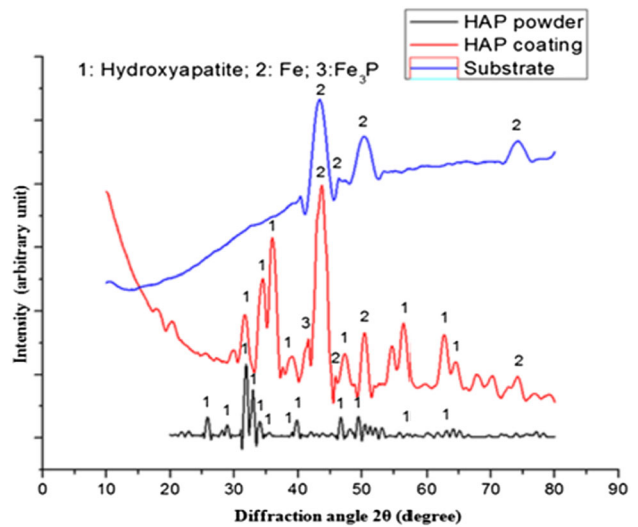


Fig. 4. XRD diffractogram of 254SS substrate, HAP powder, and HAP coating.

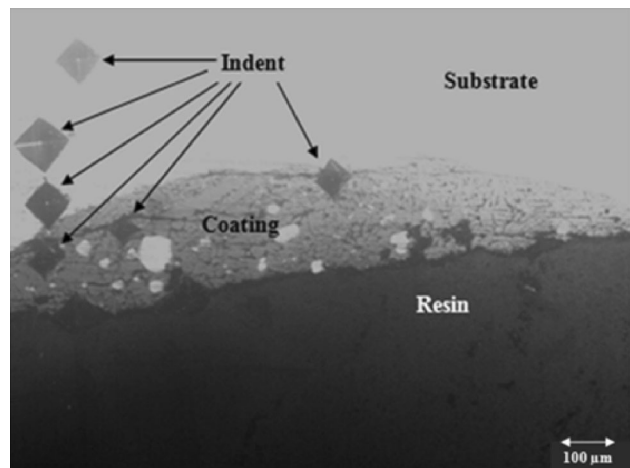


Fig. 5. Optical micrograph of the HAP-coated 254SS sample after microhardness test.

Antibacterial Efficacy

The in vitro antibacterial efficacy of the bare and HAP-coated 254SS samples was investigated against *Escherichia coli* by using the previously used FACS technique.³⁷ This is to confirm the reattainment of the antibacterial property in HAP coatings synthesized by LRM. Compared with the bare 254SS implant surface, the surface morphology of the composite layer of HAP produced on the implant surface helps in preventing bacterial attachment. This results in reduced bacterial infection, as confirmed by the FACS results and the literature.¹ Figures S7 to S10 in the supplementary material show the FACS graphs that represent the relative data of *E. coli* death, i.e., 32.2% for the HAP-coated 254SS sample, with respect to the bare 254SS sample.

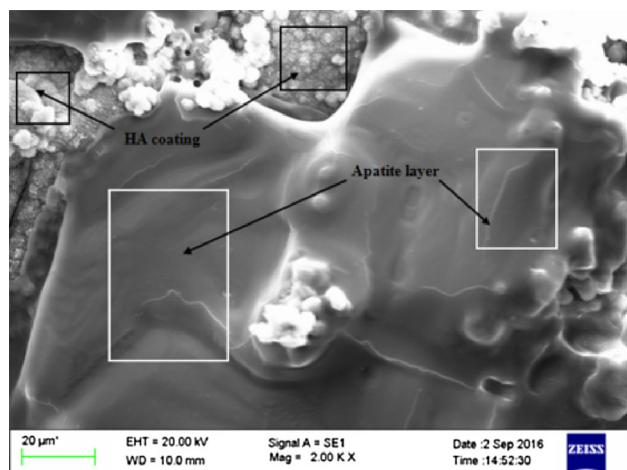


Fig. 6. SEM micrograph of HAP-coated 254SS sample after immersion test.

The main influencing factor in reducing bacterial infection is the increased surface roughness. As previously reported in the literature,³⁸ the antibacterial effect can be put down to the scale of surface irregularities, which are comparable with the size of bacteria. The higher roughness seems to limit the anchoring points for bacteria and reduces the area in contact with their membrane.³⁸

Bioactivity

The bioactivity of HAP-coated 254SS substrate was examined by conducting an immersion test in SBF. Figure 6 shows the surface morphology of the HAP-coated substrate after immersion in SBF. The growth of apatite layers is clearly visible after the immersion test, resulting in an average increase of nearly 0.16% in the weight of HAP-coated substrate.³⁹

The overall results of the present research confirm that coating of HAP on 254SS by LRM is useful for orthopedic implant applications. It overcomes the limitations of plasma-sprayed HAP coatings, such as poor bonding strength and wear resistance.

CONCLUSION

In this research, a successful attempt has been made to treat the surface of 254SS, a high nitrogen stainless steel, with HAP using an LRM system. The coatings showed a composite microstructure with austenite dendrites and interdendritic HAP with small traces of Fe₃P phase. A Vickers microhardness test confirms the higher hardness of HAP-coated 254SS substrate than that of the bare 254SS substrate. FACS tests confirm that the coated samples have a superior antibacterial property when compared with the pristine samples. An SBF immersion test confirms the rapid formation of apatite on the HAP-coated surface. The present research ably demonstrates that it is feasible to synthesize multifunctional orthopedic coatings that

can prevent infection while still promoting osseointegration on 254SS implant surfaces using the LRM additive manufacturing process.

ACKNOWLEDGEMENTS

The use of synthesis, testing, and characterization facilities of RRCAT, Indore (through Dr. C. P. Paul), IIT Kanpur, CIR (through Dr. Naresh Kumar), CMDR, Biotechnology and Applied Mechanics Departments, MNNIT Allahabad, are gratefully acknowledged. The authors would like to thank the Ministry of Human Resource Development, Government of India, and the University of Johannesburg, South Africa, for providing financial support.

OPEN ACCESS

This article is distributed under the terms of the Creative Commons Attribution 4.0 International License (<http://creativecommons.org/licenses/by/4.0/>), which permits unrestricted use, distribution, and reproduction in any medium, provided you give appropriate credit to the original author(s) and the source, provide a link to the Creative Commons license, and indicate if changes were made.

ELECTRONIC SUPPLEMENTARY MATERIAL

The online version of this article (doi:10.1007/s11837-017-2529-x) contains supplementary material, which is available to authorized users.

REFERENCES

1. S. Kurtz, K. Ong, E. Lau, F. Mowat, and M. Halpern, *J. Bone Jt. Surg. Am.* 89, 780 (2007).
2. K.J. Bozic, S.M. Kurtz, E. Lau, K. Ong, V. Chiu, T.P. Vail, H.E. Rubash, and D.J. Berry, *Clin. Orthop. Relat. Res.* 468, 45 (2010).
3. K.J. Bozic, S.M. Kurtz, E. Lau, K. Ong, T.P. Vail, and D.J. Berry, *J. Bone Jt. Surg. Am.* 91, 128 (2009).
4. J. Raphael, M. Holodniy, S.B. Goodman, and S.C. Heilshorn, *Biomaterials* 84, 301 (2016).
5. J.A. Disegi and L. Eschbach, *Injury* 31, D2 (2000).
6. J. Walczac, F. Shahgaldi, and F. Heartley, *Biomaterials* 19, 229 (1998).
7. M.L.C.A. Afonso, J.R.F.V. Villamil, E.P.G. Areas, M.R. Capri, E. Oliveira, and S.M.L. Agostinho, *Colloids Surf. A* 317, 760 (2008).
8. M.L.C.A. Afonso, R.F.V.V. Jaimes, P.A.P. Nascente, S.O. Rogero, and S.M.L. Agostinho, *Mater. Lett.* 148, 71 (2015).
9. K.D. Groot, R. Geesink, C.P. Klein, and P. Serekian, *J. Biomed. Mater. Res.* 21, 1375 (1987).
10. C.P.O. Ossa, S.O. Rogero, and A.P. Tschiptschin, *J. Mater. Sci. Mater. Med.* 17, 1095 (2006).
11. D.M. Liu, Q. Yang, and T. Troczynski, *Biomaterials* 23, 691 (2002).
12. D. Liu, K. Savino, and M.Z. Yates, *Surf. Coat. Technol.* 205, 3975 (2011).
13. D.T.M. Thanh, P.T. Nam, N.T. Phuong, L.X. Que, N.V. Anh, T. Hoang, and T.D. Lam, *Mater. Sci. Eng. C* 33, 2037 (2013).
14. J. Sun, Y. Han, and X. Huang, *Surf. Coat. Technol.* 201, 5655 (2007).
15. M.S. Kim, J.J. Ryu, and Y.M. Sung, *Electrochem. Commun.* 9, 1886 (2007).

16. Y. Huang, Y. Wang, C. Ning, K. Nan, and Y. Han, *Biomed. Mater.* 2, 196 (2007).
17. K. Nan, T. Wu, J. Chen, S. Jiang, Y. Huang, and G. Pei, *Mater. Sci. Eng. C* 29, 1554 (2009).
18. Q. Bao, C. Chen, D. Wang, Q. Ji, and T. Lei, *Appl. Surf. Sci.* 252, 1538 (2005).
19. H. Khandelwal, G. Singh, K. Agrawal, S. Prakash, and R.D. Agarwal, *Appl. Surf. Sci.* 265, 30 (2013).
20. V. Nelea, C. Morosanu, M. Ilescu, and I.N. Mihailescu, *Surf. Coat. Technol.* 173, 315 (2003).
21. K.A. Khor, P. Cheang, and Y. Wang, *JOM* 49, 51 (1997).
22. E. Bouyer, F. Gitzhofer, and M.I. Boulos, *JOM* 49, 58 (1997).
23. S.F.J. Garcia, M.B. Mayor, J.L. Arias, J. Pou, B. Leon, and A.M. Perez, *J. Mater. Sci. Mater. Med.* 8, 861 (1997).
24. M. Tlotleng, E. Akinlabi, M. Shukla, and S. Pityana, *Mater. Sci. Eng. C* 43, 189 (2014).
25. K. Balani, D. Lahiri, A.K. Keshri, S.R. Bakshi, J.E. Tercero, and A. Agarwal, *JOM* 61, 63 (2009).
26. S. Bajpai, A. Gupta, S.K. Pradhan, T. Mandal, and K. Balani, *JOM* 66, 2095 (2014).
27. S. Singh, R.M. Kumar, K.K. Kuntal, P. Gupta, S. Das, R. Jayaganthan, P. Roy, and D. Lahiri, *JOM* 67, 702 (2015).
28. J.H.C. Lin, M.L. Liu, and C.P. Ju, *J. Mater. Sci. Mater. Med.* 5, 279 (1994).
29. M. Roy, V.K. Balla, A. Bandyopadhyay, and S. Bose, *Adv. Eng. Mater.* 12, B637 (2010).
30. A. Bandyopadhyay, V.K. Balla, M. Roy, and S. Bose, *JOM* 63, 94 (2011).
31. R. Wolkowicz, *Fluorescence-Activated Cell Sorting, Brenner's Encyclopedia of Genetics*, 2nd ed. (Waltham, MA: Academic Press, 2013), p. 4368.
32. J.A. Burdick and R.L. Mauck, eds., *Biomaterials for Tissue Engineering Applications: A Review of the Past and Future Trends* (New York: Springer, 2011), p. 563.
33. M. Das, D. Basu, I. Manna, T.S.S. Kumar, and A. Bandyopadhyay, *Scr. Mater.* 66, 578 (2012).
34. V.K. Balla, A. Bhat, S. Bose, and A. Bandyopadhyay, *J. Mech. Behav. Biomed. Mater.* 6C, 9 (2012).
35. V.K. Balla and A. Bandyopadhyay, *Surf. Coat. Technol.* 205, 2661 (2010).
36. V.K. Balla, M. Das, S. Bose, G.D. Janaki Ram, and I. Manna, *Mater. Sci. Eng. C* 33, 4594 (2013).
37. A. Das and M. Shukla, *J. Mater. Des. Appl.* (2016). doi:[10.1177/1464420716663029](https://doi.org/10.1177/1464420716663029).
38. S. Bagherifard, D.J. Hickey, A.C. de Luca, V.N. Malheiro, A.E. Markaki, M. Guagliano, and T.J. Webster, *Biomaterials* 73, 185 (2015).
39. H.C. Man, K.Y. Chiu, F.T. Cheng, and K.H. Wong, *Thin Solid Films* 517, 5496 (2009).